Granular Matter (2022) 24:58
https://doi.org/10.1007/s10035-022-01219-5

ORIGINAL PAPER

Compaction of bi-dispersed granular packing: analogy with chemical thermodynamics

Ching S. Chang[1] · **Yibing Deng**[1,2]

Received: 30 June 2021 / Accepted: 9 February 2022

Abstract

The study of particle-packing models for bi-dispersed packings is important in the field of granular materials, from both theoretical and practical perspectives. Several particle-packing models have been developed for predicting the packing density (or specific volume) of a bi-dispersed packing. Most of the currently available models are phenomenological, which predict the specific volumes of a bi-dispersed packing as a function of fraction of species, and have applied to various fields, such as in concrete, pharmaceutical, soil engineering, etc. In this study, we analyze the packing densities of granular mixtures using an analogy to the thermodynamic theory for chemical solutions. The thermodynamic theory for chemical solutions provides the connections among the bulk solution density, the chemical interaction activities between species, and the concentration of each species in the solution. Parallel to the chemical potential of each species in the solution, we introduce an "excess free volume potential" for each granular species. With the interaction activities of two species in a bi-dispersed granular system, we explain the volume compaction behavior of a granular system from a new context. Subsequently, using the second law of thermodynamics, an analytical method is proposed to quantify the excess free volume potentials and to predict the density of a granular mixture. The developed analytical method is then validated by the experimental results of bi-dispersed packing mixtures of glass beads and silica sands. The performance of the analytical method and its validity are demonstrated.

Keywords Binary granular system · Thermodynamics · Analytical method · Compaction

List of symbols

Packing descriptors

V	Total volume of a bi-dispersed packing
υ	Specific volume of a bi-dispersed packing
V_1^0, V_2^0	Total volumes of each component in mono-dispersed packing state
$\upsilon_1^0, \upsilon_2^0$	Specific volumes of each component in mono-dispersed packing state
N_1, N_2	Total number of large particles and small particles in a bi-dispersed packing
y_1, y_2	Solid volume fraction of each component in a bi-dispersed packing
$\mathrm{v}_1^g, \mathrm{v}_2^g$	Particle solid volume of each component in a bi-dispersed packing
d_1, d_2	Particle size of each component in a bi-dispersed packing
$\mathrm{v}_1^m, \mathrm{v}_2^m$	Particle volume potential of the mth particle of each component in a bi-dispersed packing
$\mathrm{v}_1^0, \mathrm{v}_2^0$	Average particle volume potential of each component in mono-dispersed packing state
$\mathrm{v}_1, \mathrm{v}_2$	Average particle volume potential of each component in a bi-dispersed packing

Thermodynamics terms

X	Compactivity (granular temperature)
S	Granular entropy
V', V	Internal volume potential, Gibbs volume potential
ζ	Extent of reaction
ΔV	Excess free volume potential of the bi-dispersed packing
$\Delta \mathrm{v}_1, \Delta \mathrm{v}_2$	Excess free volume potential for each component in a bi-dispersed packing

---

✉ Ching S. Chang
cchang@engin.umass.edu

Yibing Deng
yibingdeng@outlook.com

[1] Department of Civil and Environmental Engineering, University of Massachusetts, Amherst, MA 01003, USA

[2] Department of Municipal and Ecological Engineering, Shanghai Urban Construction Vocational College, Shanghai 200438, China

α_1, α_2	Interaction activity coefficients for each component in a bi-dispersed packing
r_i	Particle size ratio
$\eta_1, \eta_2(\eta)$	Material parameter for each component (averaged value)
$\bar{x}$	Internal state variable

1 Introduction

This paper deals with a simple, yet fundamental, phenomenon in the physics of granular materials: granular compaction. A packing of grains in a container gets more and more compact under gentle shaking or tamping. Under continuous shaking or tamping, a stationary state of volume is eventually established at equilibrium. In this paper, we focus on the volume characteristics of a bi-dispersed granular packing in a stationary state.

Compaction of bi-dispersed granular packings is related to both practical and basic scientific problems, which has been broadly studied for design and manufacturing in many fields, such as mineral, metallurgical, pharmaceutical, and geotechnical industries [28, 33, 43, 46]. It can be generally observed that packing density varies with the fraction of species in a bi-dispersed packing. Interestingly, the change of density with respect to the fraction of species is non-monotonic, exhibiting a peak at a specific fraction of species.

Since these issues are shared in technological applications, many phenomenological models have been developed for predicting densities of bi-dispersed packings of various types of grains [10, 17, 19, 27, 35, 48, 53, 60, 61]. These models require two to four material parameters.

With the rapid advances in computer technology, the method of computer simulation has progressed significantly. Computer simulation has been applied by many researchers for studying geometric packing properties of polydisperse granular material (e.g., [20, 31, 45, 56, 58]). Many studies have been devoted specifically to the geometric properties and the bulk mechanical properties of bi-dispersed packing (e.g., [1, 18, 25, 34, 40, 50, 55]). Packing structural characteristics of bi-dispersed mixtures have been investigated by computer simulation [13, 29, 38, 49].

A theoretical approach for bi-dispersed packing of spheres was developed by Danisch et al. [16] based on the formalism of Edwards' statistical mechanics approach. However, the method requires a partition function to describe the microstate configurations, which needs to be established with the aid of numerical simulation. Thus, the method is not practically useful.

We intend to develop a novel approach to study the bi-dispersed granular packings, along the lines of analyzing mixed chemical solutions using the principles in thermodynamics. Due to the nature of granular material as a non-chemical and athermal material, classic thermodynamics is not applicable to the analysis of granular materials. Therefore, in the spirit of Edwards' granular temperature approach, we suggest that both the thermal and chemical potentials (i.e., internal energy) be replaced by the volume potential of the granular system. Hopefully, it opens the door for applying thermodynamics concepts of chemical solutions to the analysis of granular mixtures. The challenge is to establish the analogy between the chemical potential of a mixed solution and the volume potentials of species in a bi-dispersed granular packing.

In the next section, we first propose a fundamental equation that extends Edwards approach by analogously replacing not only the thermal energy but also the chemical potential with the volume potentials of a granular equilibrium system. We then explain the modeling approach, which is similar to the formalism of equilibrium thermodynamics used in chemical solutions. In Sect. 3, using Euler's theorem, we characterize a bi-dispersed packing by two volume potentials, each corresponding to a species of particles. In Sect. 4, we formulate an equation that prescribes the excess free volume (in analogy to the Gibbs excess free energy) for a granular packing based on the interaction activities between the two species of particles. In Sect. 5, we study the experimentally observed behavior of interaction activities. In Sect. 6, we introduce an internal state variable, which represents the state of the packing configuration, and hypothesize an equation that defines a relationship between the internal state variable and the excess free volume potential. Applying the thermodynamics law of equilibrium, the internal state variable can be determined from the composition of the packing mixture. In Sect. 7, we summarize the proposed model, which is then validated by experimental results from mixtures of glass beads and silica sands in Sects. 8 and 9.

2 Approach of this paper

2.1 Connection to thermodynamics

Granular media, such as powders or sands, are made of discrete particles of size larger than 100 μm, which often interact only through dissipative contact forces. Without an external drive, their kinetic energy is rapidly lost, thus the granular media is referred to as a non-thermal system. Due to the insignificance of their thermal energy in comparison to the energy needed to move a grain, classic thermodynamics is not useful for the analysis of granular material.

Edwards [21] suggested that, due to the dissipative nature of granular systems, the role of the conserved quantity should be played by the volume V of the system instead of the internal energy U [8, 22, 23]. The Edwards approach has been verified for granular systems by many investigators (e.g. [2, 15, 44], etc.).

Assuming equiprobability exists for microstate configurations of the system, Edwards defined a configurational "granular entropy S", which is proportional to the logarithm of the number of mechanically stable microstates at a given volume. Instead of the temperature T, he also introduced a "granular temperature X", named compactivity. Thus, in analogy to the expression in classical thermodynamics, $dU = \mathrm{T}dS$, the compactivity is, therefore, related to the volume dependence of the entropy for a non-thermal granular system, given by $dV = \mathrm{X}dS$ [23]. Based on this concept, the granular system can be analyzed by a statistical mechanical formalism in much the same way that is done for a thermodynamics system.

This statistical mechanical formalism has been successfully applied to study the mechanical response at the jamming and its transition of granular matter and provided understanding about the nature of granular medium in solid, fluid, and gas phases [5, 32, 39, 42, 52].

The Edwards statistical mechanical formalism has also been applied to predict the compacted density for bi-dispersed mixtures of particles [16]. The key idea is to establish a partition function that prescribes the volumes at microstate so that a mean-field theory can then be used to calculate the density of the bi-dispersed mixture. However, the partition function needs to be established with the aid of numerical simulation. This limits much of the analysis to numerical evaluation of the expectation values. Although the method is fundamentally sound, it is practically not useful.

In this paper, we do not use the Edwards statistical mechanical formalism. Instead, we extend Edwards approach by analogously replacing not only the thermal energy but also the chemical potential with the volume potentials of a granular equilibrium system. Thus, the fundamental equation becomes:

$$dV' = XdS + \sum_{1}^{N} \mathrm{v}_i dN_i \tag{1}$$

Parallel to "internal energy", V' can be termed "internal volume potential". The second term on the right side of the equation is analogous to the chemical potential. The symbol N_i is the number of particles for the ith species in the system, and v_i is the volume potential of the ith species. Equation (1) shows that, there is a contribution v_i d N_i for each species to the total volume in a bi-dispersed granular system.

Because the entropy is not easily measured experimentally, for convenience, we apply the Legendre transformation to the internal volume potential V' in Eq. (1), and we define a "Gibbs volume potential" $V = V' - XS$ in analogous to Gibbs energy, then Eq. (1) becomes

$$dV = -SdX + \sum_{1}^{N} \mathrm{v}_i dN_i \tag{2}$$

At constant value of the intensive property X (i.e., $dX = 0$), Eq. (2) can be integrated to obtain

$$V = \sum_{1}^{N} \mathrm{v}_i N_i \tag{3}$$

The Gibbs volume potential V is a more useful property because, in this study on compaction of a bi-dispersed packing, the packing preparation procedure can be controlled experimentally. For the condition of $dX = 0$, the volume potential V achieved under compaction for a bi-dispersed packing is expressed as:

$$V = \mathrm{v}_1 N_1 + \mathrm{v}_2 N_2 \tag{4}$$

The average volume potential of a large particle is referred to as v_1 and the average volume potential of a small particle is referred to as v_2. In this paper, for convenience, the particle volume potential will always refer to the average particle volume potential. The value N_1 is the total number of large particles, and N_2 is the total number of small particles.

2.2 Descriptors of a bi-dispersed packing

A bi-dispersed packing consists of two species: the large-particle group with particle size d_1, and the small-particle group with particle size d_2. Their corresponding solid particle volumes are v_1^g and v_2^g. The composition of the packing is described by the number of particles of the two species N_1 and N_2. The total volume of solid for the packing is $\mathrm{v}_1^g N_1 + \mathrm{v}_2^g N_2$. The composition of a bi-dispersed packing is also commonly described by the solid volume fractions of the large and small particle groups,y_1 and y_2, given by

$$y_1 = \frac{\mathrm{v}_1^g N_1}{\mathrm{v}_1^g N_1 + \mathrm{v}_2^g N_2}; \quad y_2 = \frac{\mathrm{v}_2^g N_2}{\mathrm{v}_1^g N_1 + \mathrm{v}_2^g N_2} \tag{5}$$

The two species can be separately packed into two mono-dispersed packings with volumes V_1^0 and V_2^0. The average particle volume potentials for the two mono-dispersed packings are respectively $\mathrm{v}_1^0 = V_1^0/N_1$ and $\mathrm{v}_2^0 = V_2^0/N_2$.

The frequently used density descriptor is specific volume, which is defined as the ratio of the specimen volume to its solid volume. The specific volume υ for the packing mixture and the specific volumes,υ_1^0, υ_2^0, for the mono-dispersed packings of the two species are expressed as follows:

$$\upsilon = \frac{V}{\mathrm{v}_1^g N_1 + \mathrm{v}_2^g N_2}; \quad \upsilon_1^0 = \frac{\mathrm{v}_1^0}{\mathrm{v}_1^g}; \quad \upsilon_2^0 = \frac{\mathrm{v}_2^0}{\mathrm{v}_2^g} \tag{6}$$

It is noted that v_1^0 and v_2^0 can be directly measured from experiments, which are commonly known values for a particle mixing problem.

2.3 Modelling approach

Our objective is to derive a model that can predict the volume of a bi-dispersed mixture V with any arbitrary species fraction knowing the values of v_1^0 and v_2^0 of the mono-dispersed packings of the two species.

The volume V can be predicted by Eq. (4) if the values of particle volume potentials, v_1 and v_2, are known. However, in a bi-dispersed mixture, due to the interactions between particles of two species, the particle volume potentials v_1 and v_2 are different from the particle volume potentials (v_1^0 and v_2^0) in their mono-dispersed states. Note that the values of v_1 and v_2 are defined as the average volume potentials for particles of each species, while these particles are randomly distributed in the packing mixture. Thus, it is not only difficult to separately measure the values of v_1 and v_2 in experiments, but also a challenge to create an analytical model that can predict the values of v_1 and v_2. To achieve a prediction model, there are two types of approach:

(1) *Using the formalism of statistical mechanics* The challenge is to formulate a partition function that can adequately encompass the complex configurations of all microstates with all degrees of freedom [6]. Thus, one needs to know the complete packing configuration in detail, which is typically obtained from the computer simulation method. The microstate configurations are usually constructed based on the tessellations (Voronoi-based or quadron-based) divided from the complete packing configuration [7, 11, 51]. This approach is not practical for developing a model as a predicting tool.

(2) *Using the formalism of equilibrium thermodynamics* The challenge is to postulate an equation that defines the relationship between an internal state variable and the volume potentials of the two species. Although the internal variable typically represents a macroscopic average in some fashion of the packing configuration, it is not required to represent the complete packing configuration in detail, as long as the internal variable can reflect the relevant features of the packing configuration and provide a good correlation to the volume potentials. Thus, the postulated internal state variable must be based on physically observed behavior and be constrained by the laws of thermodynamics [14, 30, 41].

In this paper, we adopt the second approach. In the following, we investigated the physical meaning of v_1 and v_2, and their relations to the values of v_1^0 and v_2^0.

3 Assessment of partial volume potential

Since the volume V of a granular system is an *extensive* variable, which is homogeneous of degree 1, thus according to Euler's theorem, the total volume of a mixture is

$$V\left(N_1, N_2\right) = N_1\left(\frac{\partial V}{\partial N_1}\right) + N_2\left(\frac{\partial V}{\partial N_2}\right) \tag{7}$$

Comparing Eq. (7) with Eq. (4), the volume potential $\mathrm{v}_i = \partial V/\partial N_i$. Thus, Eq. (7) provides a method of interpreting the volume potential v_i of each species from several experimentally measured V for bi-dispersed packings with various species fractions y_1 and y_2. The function $V(y_1, y_2)$ can be numerically constructed from the experimental data. Since y_1, y_2 are related to N_1,N_2 (see Eq. 5), the function $V(y_1, y_2)$ can be converted to $V(N_1, N_2)$, and their derivatives $\partial V/\partial N_i$ can be obtained.

The definition of $\partial V/\partial N_i$ also conceptually provides a link between the volume potential v_i and the microstate configurations. The partial derivative represents the change of packing volume dV caused by mixing a small number ($\mathrm{d}\,N_i$) of particles of the *ith* species to the packing mixture while the total particle number N_j of the other species is kept constant. In order to evaluate the partial derivative, the number of particles, $\mathrm{d}\,N_i$, should be small enough from the view of calculus. Since the microstate configurations play a major role, we conceptually consider the number of particles $\mathrm{d}\,N_i$ as a single particle mixed into the packing mixture, so that we can focus on the microstate configuration of this added single particle and its neighboring particles. We repeat the single particle mixing for a large number (M) of times and obtain a large set of microstate configurations.

For the mth trial, the single particle occupies a space, denoted as particle volume v_i^m. The particle volume is dependent on the location of this particle and the configuration of its surrounding particles. Based on the hypothesis that all microconfigurations are equally probable, the particle volume v_i (i.e., $\partial V/\partial N_i$ in Eq. (7)) can be regarded as the mean of the particle volume v_i^m for the M microstates.

$$\mathrm{v}_i = \frac{1}{M}\sum_{m=1}^{M} \mathrm{v}_i^m \tag{8}$$

The microstates probed by the single particle mixing process provides a method to assess the value of v_i from the view of microstate configurations. The characteristics of microstate configuration will be investigated to formulate the excess free volume potentials for each species.

4 Excess free volume potential due to interaction of species

The particle volume potential for a mono-dispersed packing v_i^0 is analogous to the chemical potential of an ideal solution. After mixing of two mono-dispersed species, the particle volume potential in the bi-dispersed packing for each species is denoted by v_i.

Analogous to the excess Gibb's free energy in the classic thermodynamics, an excess free volume potential, denoted by Δv_i, is defined as the difference between the particle volume potential v_i in a mixture and the particle volume potential v_i^0 in a mono-dispersed packing.

$$v_i = v_i^0 - \Delta v_i \zeta \tag{9}$$

The parameter ζ is the *extent of reaction*, which is between 0 and 1. In our study, we consider only the equilibrium condition of a bi-dispersed packing (i.e., $\zeta = 1$). Thus, the excess free volume at equilibrium state is $\Delta v_i = v_i^0 - v_i$.

The excess free volume Δv_i of the *ith* species, in a bi-dispersed packing, is caused by the interaction between particles of two different species. In the following, we investigated the value range of the excess free volume potentials Δv_i for each species by examining their microstate configurations.

4.1 Embedment formation of a large particle

In a bi-dispersed packing of two species (size groups of d_1 and d_2), the excess free volume Δv_1 for the large particle (species with size d_1) can be examined from the microstate configurations with a large particle at the center surrounded by its neighboring particles. The large particles can be viewed as embedded in the particle mixture; thus, it is termed as an embedment formation. The free volume of a center particle depends on the configuration of its surrounding particles. Two extremes can be observed: (1) when the neighboring particles surrounding a central large particle are all large particles, as shown in Fig. 1a, the particle volume potential v_2 is expected to be same as that of the mono-dispersed packing $\left(v_1 = v_1^0\right)$. (2) when the neighboring particles surrounding a central large particle are all small particles, as shown in Fig. 1b, and the small particles are sufficiently small ($d_2/d_1 \approx 0$), the void volume associated with the central particle is almost zero. The average particle volume v_1 is approximately to be the particle solid volume $\left(v_1 = v_1^g\right)$.

In a general case, the surrounding neighbor particles are bi-dispersed and d_2/d_1 is not small, then the particle volume potential v_1 is expected to be between the two extremes, i.e., $v_1^g < v_1 < v_1^0$. It can be expressed as:

$$v_1 = v_1^0 - \alpha_1(v_1^0 - v_1^g) \quad \text{or} \quad \Delta v_1 = \alpha_1(v_1^0 - v_1^g) \tag{10}$$

The activity coefficient α_1 represents the interaction activity of the large particles in the bi-dispersed packing. Its value is between 0 and 1. When $\alpha_1 = 0$, then $v_1 = v_1^0$, the particle volume potential of large particles in the bi-dispersed packing is same as that in the mono-dispersed packing. Thus, there is no interaction activity. Whereas, when $\alpha_1 = 1$, then $v_1 = v_1^g$, the particle volume potential is smaller than that in the mono-dispersed packing due to the interaction activity. The exact value of α_1 is dependent on the composition of the bi-dispersed packing (i.e., particle sizes d_1 and d_2 and particle number of each species N_1 and N_2).

4.2 Filling formation of a small particle

Now we examine the microstate configurations with a small particle at the center surrounded by its neighboring particles. The small particle can be viewed as filling in the voids of the large particles; thus, it is termed as a filling formation. The free volume of a center particle depends on the configuration of its surrounding particles. Two extremes can be observed: (1) when the neighbor particles surrounding a central small particle are all small particles, as shown in Fig. 2a, the particle volume potential v_2 is expected to be same as that of the mono-dispersed packing $\left(v_2 = v_2^0\right)$. (2) when the neighboring particles surrounding a central small particle are all large

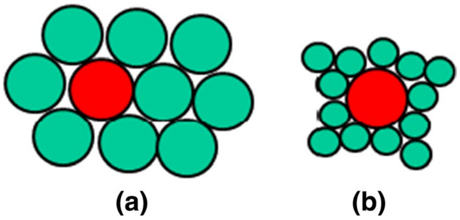

Fig. 1 Micro-configurations of a large particle surrounded by: **a** all large particles and **b** all small particles

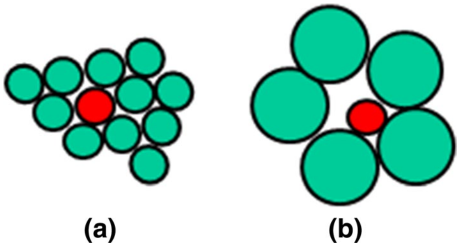

Fig. 2 Micro-configurations of a small particle surrounded by: **a** all small particles and **b** all large particles

particles, as shown in Fig. 2b, and the central small particle is sufficiently small ($d_2/d_1 \approx 0$), so that it fits into a void of surrounding large particles as a float particle, which remains mobile even though their surrounding particles are jammed (i.e., mechanical stable). These type of small particles are called rattler-particles [5]. In this case, the small particles caused no change in the packing volume, thus the particle volume potential $\mathrm{v}_2 = 0$.

Again, in a general case, if the surrounding neighboring particles are bi-dispersed and the d_2/d_1 is not small, then the particle volume potential v_2 is expected to be between the two extremes, i.e., $0 < \mathrm{v}_2 < \mathrm{v}_2^0$. It can be expressed as:

$$\mathrm{v}_2 = \mathrm{v}_2^0 - \alpha_2 \mathrm{v}_2^0 \quad \text{or} \quad \Delta \mathrm{v}_2 = \alpha_2 \mathrm{v}_2^0 \tag{11}$$

The activity coefficient α_2 represents the interaction activity of the small particles in the bi-dispersed packing. Its value is also between 0 and 1, depending on the composition of the bi-dispersed packing.

Based on Eqs. (10) and (11), the total volume of a bi-dispersed packing can be further derived as a function of the activity coefficients α_1 and α_2.

$$V = \mathrm{v}_1 N_1 + \mathrm{v}_2 N_2 = \left(\mathrm{v}_1^0 - \alpha_1(\mathrm{v}_1^0 - \mathrm{v}_1^g)\right)N_1 + \mathrm{v}_2^0\left(1 - \alpha_2\right)N_2 \tag{12}$$

In Eq. (12), v_1^0 and v_2^0 are known values for mono-dispersed packings. The value of v_1^g, N_1, N_2 are the known composition of the packing. Thus, the activity coefficients α_1 and α_2 are the only unknowns, which are essential parameters for a quantitative prediction of the volume of a bi-dispersed packing.

5 Activity coefficients

5.1 Experiments used to interpret the activity coefficients

The activity coefficients are dependent on the microstate configurations of particles, which are influenced by two main factors: the relative particle sizes (or the particle size ratio d_2/d_1) and the species fractions of the bi-dispersed packing. The influences of these two factors are examined in this section using the experimentally measured results on glass beads reported by Kwan et al. [35]. In their experiments, four different particle size groups were selected with sizes d (mm) = 1.43, 3.29, 5.26, 11.71. The measured particle volume potential v_i^0 for these four mono-dispersed packing are (1.652, 1.672, 1.68, 1.706). The four particle groups were mixed into three bi-dispersed systems denoted by size combinations (d_1, d_2): (3.29, 1.43), (5.26, 1.43), and (11.74, 1.43). Each system has 9 combinations of species-fractions (i.e., the fractions of small particles y_2 varies from 0.1 to 0.9). All bi-dispersed samples were compacted using the same packing procedure specified in British Standard [9].

Following the procedure described in Sect. 3, we interpret the particle volume potentials v_1 and v_2 from the measured specific volumes υ of the bi-dispersed packings of glass beads. First, the function $\upsilon(\mathrm{y}_1, \mathrm{y}_2)$ can be numerically constructed and converted to $V(\mathrm{N}_1, \mathrm{N}_2)$. Next, for each bi-dispersed packing, the particle volume potentials v_1 and v_2 (i.e., $\partial V/\partial N_1$ and $\partial V/\partial N_2$) can be computed. Then, from Eqs. (10) and (11), values of the activity coefficients α_1 and α_2 can be calculated for each bi-dispersed packing and plotted in Fig. 3.

Figure 3 shows that the activity coefficients α_1 and α_2 are significantly influenced by both size ratio and species fractions. To separate the influence of these two factors, we first eliminate the factor of species fraction. In the

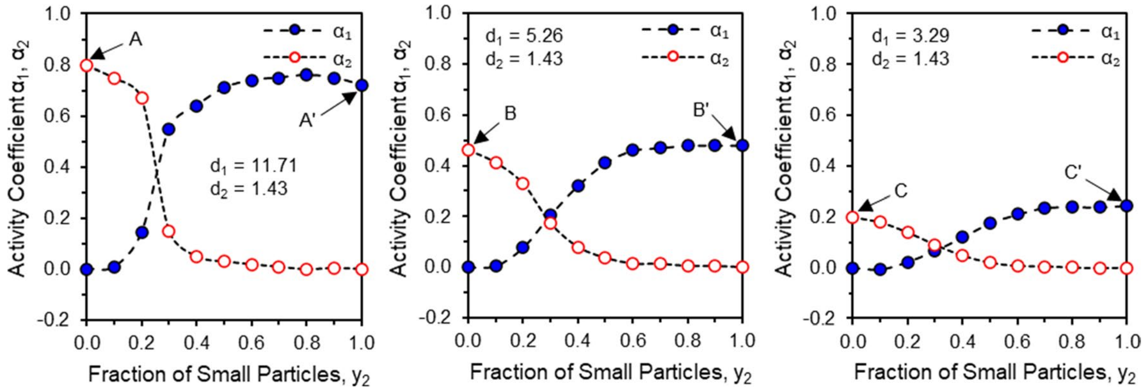

Fig. 3 The activity coefficients α_1 and α_2 interpreted from experimental results for bi-dispersed packings with three size ratios

measured results shown in Fig. 3, we select two specific conditions (fractions $y_2 = 0$, and $y_2 = 1$). For the $y_2 = 0$ condition, the coefficient α_2 represents the interaction activity of a few small particles in a mono-dispersed packing of large particles. Whereas, for the $y_2 = 1$ condition, the coefficient α_1 represents the interaction activity of a few large particles in a mono-dispersed packing of small particles. In both cases, the packing mixtures are termed dilute granular mixtures (an analogy to the dilute chemical solutions.)

5.2 The interaction activity of a species in a dilute granular mixture

The activity coefficients α_1 and α_2 at the two specific conditions (fractions $y_2 = 0$, and $y_2 = 1$) correspond to the six points (A, B, C, A', B', C') shown in Fig. 3.

(1) $y_2 = 1$: The three points (A', B', C') represent the α_1 of three packing mixtures: each packing mixture corresponds to a few particles of size d_1 (d_1=3.29, 5.26, 11.71 mm) in a mono-dispersed base packing with particle size $x = 1.43$ mm. Note that for all three packing mixtures, the microstate configurations are in embedment formation (i.e., the microstate configuration resembles a large particle surrounded by all small particles). The activity coefficient of the large particles α_1 for the three cases are plotted against the size ratio $r_1 = x/d_1$ in Fig. 4.

(2) $y_2 = 0$: The three points (A, B, C) represent the α_2 of three mixtures: each packing mixture corresponds to a few particles of size $d_2 = 1.43$ mm in a mono-dispersed base packing with particle size x (x=3.29, 5.26, 11.74 mm). In all three packing mixtures, the microstate configurations are in filling formation (i.e., the microstate configuration resembles a small particle surrounded by all large particles). The activity coefficient of the small particles α_2 for the three cases are plotted against the size ratio $r_2 = d_2/x$ in Fig. 4.

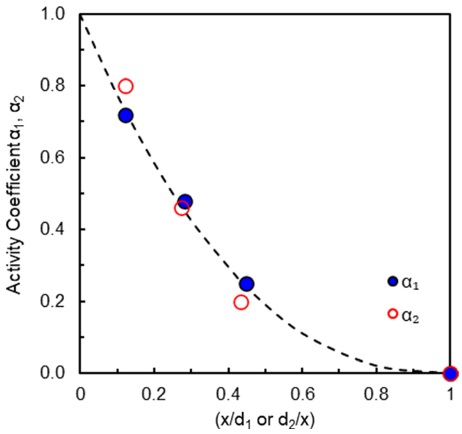

Fig. 4 Activity coefficients versus size ratios x/d_1 or d_2/x. The variable x is the particle size of mono-dispersed base packings in the dilute mixture

Figure 4 show in which the interaction activity of a species is dependent on the particle size ratio of the two species. A higher size ratio indicates a greater difference in the volume potentials between the two species, thus leads to higher interaction activity. Species in chemical solutions are not classified by sizes. However, the same principle also applies in chemical solutions that a greater difference in the chemical potentials between the two species of molecules leads to higher interaction activity.

The data points in Fig. 4 fit well to a power law, given by

$$\alpha_i = \left(1 - r_i\right)^{\eta_i} \quad (i = 1, 2) \tag{13}$$

For the two activity coefficients α_1 and α_2, Eq. (13) represents respectively,

$$\alpha_1 = \left(1 - \frac{x}{d_1}\right)^{\eta_1}; \quad \alpha_2 = \left(1 - \frac{d_2}{x}\right)^{\eta_2} \tag{14}$$

The experimental data in Fig. 4 shows that the two curves are nearly identical. The fitted values of exponents are nearly the same (i.e., $\eta_1 = \eta_2 = \eta = 2.4$).

5.3 The interaction activity of a species in a concentrated granular mixture

In Fig. 3, except the two specific conditions mentioned above, all data points are considered as concentrated granular mixtures (analogous to concentrated chemical solution). All activity coefficients, α_1 and α_2, are significantly influenced by both factors: species-fractions and particle size ratio. For bi-dispersed packings with a given size ratio, the values of α_1 and α_2 vary opposite in trends with respect to the fraction of small particles y_2, thus they are negatively correlated. The influences for these two factors (size ratio and fractions) are compounded and not easy to phenomenologically describe. Therefore, it is desirable to have a theoretical model to predict the interaction activities of species due to the combined influences.

For a chemical solution of known concentration, the exact elements of substances and their free energies are known precisely. Therefore, the interaction activities of species in the solution can be theoretically determined [4, 26, 47]. Obviously, the theory of chemical solution is not applicable to granular material. However, although there is no chemical reaction between granular particles, the analogous particle volume potentials interact in a similar way to that of chemical potentials between species. Thus, the activity coefficients of a granular mixture can be analyzed based on the principle of potential balance between the two species. Here, we attempt to develop an innovative model that can be used to determine the activity coefficients α_1 and α_2 for granular mixtures based on the balance of volume potentials of the two granular species at equilibrium.

6 Internal state variable

6.1 Connection between internal state variable and particle volume potentials

The challenge is to postulate a relationship between an internal state variable and the particle volume potentials of the two species. Although the internal variable typically represents a macroscopic average in some fashion of the packing configuration, it is not required to represent the complete packing configuration in detail, as long as the internal variable can reflect the relevant features of the packing configuration and provide a good correlation to the volume potentials. Thus, the postulated internal state variable must be based on physically observed behavior and constrained by the laws of thermodynamics.

Since the activity coefficients are dependent on the configuration of the packing mixture, we first hypothesize an internal variable, which represent the packing configuration, and then we postulate an equation that defines the relationship between the activity coefficients and the internal state variable. Our purpose is to hypothesize a simple form of internal state variable while it still can reflect the relevant features of the packing configuration, so that the postulated equation is general enough to encompass the relevant material behaviors to be predicted.

The postulated internal state variable $\bar{x}$ is a scaler with a unit of length. The physical meaning of $\bar{x}$ can be regarded as the *effective particle size* of the bi-dispersed packing (i.e., the bi-dispersed packing is regarded as a mono-dispersed packing with particle size $\bar{x}$). We hypothesize that, in a bi-dispersed packing, the activity coefficient of a species is related to the two particle sizes d_1, d_2 and the effective particle size $\bar{x}$ in the same form as Eq. (14), except that the particle size x for the mono-dispersed packing is replaced by the effective particle size $\bar{x}$ of the bi-dispersed packing. Thus, the activity coefficients for the two species are linked to the variable $\bar{x}$ by:

$$\alpha_1 = \left(1-\frac{\bar{x}}{d_1}\right)^{\eta}; \quad \alpha_2 = \left(1-\frac{d_2}{\bar{x}}\right)^{\eta} \tag{15a, b}$$

Note that the activity coefficients of both species refer to the same packing mixture (i.e., the same state variable $\bar{x}$). Thus, the activity coefficients are correlated through the same variable $\bar{x}$. In this way, when the value of α_1 is high, the value of α_2 is low, and vice versa. The postulated equation provides a negative trend of correlation between α_1 and α_2.

Since the value of α_i is between 0 and 1, the value of $\bar{x}$ for a bi-dispersed packing is within the range of $d_1 \geq \bar{x} \geq d_2$. Using Eq. (15a or 15b), the exact values of $\bar{x}$ can be back calculated from the measured α_1 or α_2 for the bi-dispersed packings with various species fractions. The values of $\bar{x}$, calculated using the measured α_1 or α_2 displayed in Fig. 3, are plotted in Fig. 5. For each species fraction, two different values $\bar{x}$ can be back calculated: one from Eq. (15a) and the other from Eq. (15b). The range of calculated $\bar{x}$ is shown as the shaded zone in Fig. 5.

The shaded zone between the two values is very narrow, indicating that a single value of $\bar{x}$ can be used to calculate both coefficients. In Fig. 5, the range of fractions y_2 can be classified into three regions: (I) the large particles dominant region, (II) the transitional region, and (III) the small particles dominant region. In the first region, the fraction of small particles y_2 is small and the effect particle size $\bar{x} \approx d_1$. The large particles are connected in direct contact, and the microstate configurations are dominant by the filling formation. As the fraction y_2 increases, in the second region, the small particles fill most of the void space between the large particles and start to separate the

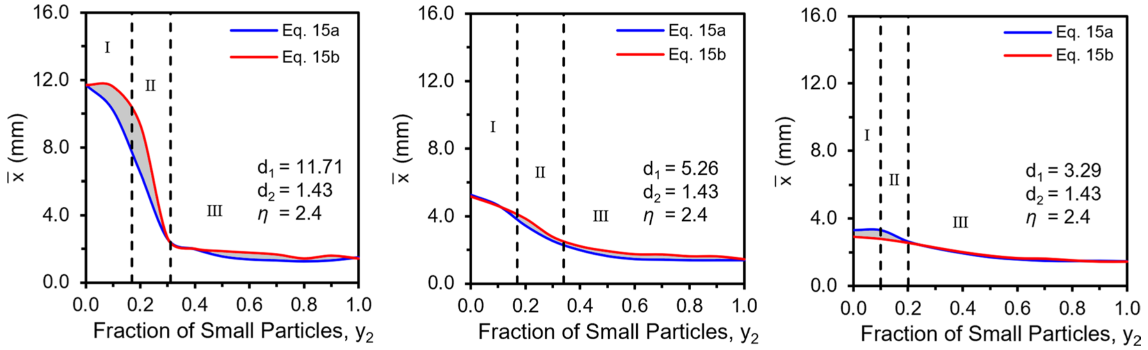

Fig. 5 Effective particle size $\bar{x}$ back calculated from activity coefficients for bi-dispersed packings with three size ratios. The range of fractions y_2 is classified into three regions: (I) the large particles dominant region, (II) the transitional region, and (III) the small particles dominant region

direct contact of the large particles. In the third region, the fraction y_2 continues to increase. The separated and isolated large particles are now embedded in the matrix formed by small particles, resulting in a microstate configuration that is dominant by small particles.

Substituting the value range of $\bar{x}$ shown in Fig. 5 to Eq. (15a) and Eq. (15b), the calculated range of activity coefficients are plotted and shown as the shaded zones in Fig. 6. The good agreement between the shaded zones and the experimentally obtained data also indicates that, for a given packing mixture, a single value of $\bar{x}$ is sufficient to model the activity coefficients of both species.

6.2 Second law and criterion for achieving equilibrium

As described previously, the internal state variable $\bar{x}$ can be back calculated from activity coefficients but cannot be obtained directly from the composition of the bi-dispersed packing. Thus, for modeling purposes, the variable $\bar{x}$ is not known priori and needs to be determined theoretically. In Eq. (15), the particle volume potentials of both species are governed by the value of $\bar{x}$. Thus, $\bar{x}$ must be constrained so that the equilibrium of the two potentials is achieved. According to the second law of thermodynamics, equilibrium is achieved when the excess free energy is minimized (i.e., $dG^E \leq 0$) for any process in an isolated system. Analogous to this notion, in our formulation, the excess free volume potential must be minimized at system equilibrium. Based on Eqs. (10) and (11), the excess free volume potential can be written as

$$\Delta V(\bar{x}) = \sum_{i=1}^{2} (\mathrm{v}_i^0 - \mathrm{v}_1)\mathrm{N}_i \tag{16}$$

Using the complete expression of the excess free volume potentials in Eqs. (10) and (11), Eq. (16) can be further expressed in terms of activity coefficients.

$$\Delta V(\bar{x}) = \sum_{i=1}^{2} \Delta \mathrm{v}_i \mathrm{N}_i = \alpha_1(\bar{x})(\mathrm{v}_1^0 - \mathrm{v}_1^g)N_1 + \alpha_2(\bar{x})\mathrm{v}_2^0 N_2 \tag{17}$$

For the excess free volume potential $\Delta V(\bar{x})$, at constant packing composition N_1, N_2, the equilibrium condition can be achieved by, $\frac{\partial \Delta V(\bar{x})}{\partial \bar{x}} = 0$, which leads to $\mathrm{N}_1 \frac{\partial \mathrm{v}_1}{\partial \bar{x}} + \mathrm{N}_2 \frac{\partial \mathrm{v}_2}{\partial \bar{x}} = 0$. The two terms in this equation can be regarded as two thermodynamic forces, and the zero sum of the two forces assures the condition of equilibrium.

The equilibrium condition can also be written in terms of activity coefficients based on Eq. (17), so that the relation between the two activity coefficients α_1 and α_2 is given by

$$\frac{\partial \alpha_1(\bar{x})}{\partial \bar{x}}(\mathrm{v}_1^0 - \mathrm{v}_1^g)N_1 + \frac{\partial \alpha_2(\bar{x})}{\partial \bar{x}}\mathrm{v}_2^0 N_2 = 0 \tag{18}$$

The two terms in Eq. (18) can also be regarded as two thermodynamic forces. The relationship between α_1 and α_2 is obtained by seeking the balance of these two forces.

In the three equations, Eq. (15a), Eq. (15b) and Eq. (18), the variables v_1^0, v_2^0, v_1^g, N_1 and N_2 are known constants. The three unknowns $\bar{x}$, α_1 and α_2 can then be solved by the three equations. With the solved activity coefficients α_1 and α_2, the volume potentials v_1 and v_2 for each species can be obtained by Eqs. (10) and (11). The total volume of the packing mixture can be determined by (see Eq. (12))

$$V = \left(\mathrm{v}_1^0 - \alpha_1(\mathrm{v}_1^0 - \mathrm{v}_1^g)\right)N_1 + \left(\mathrm{v}_2^0 - \alpha_2 \mathrm{v}_2^0\right)N_2. \tag{19}$$

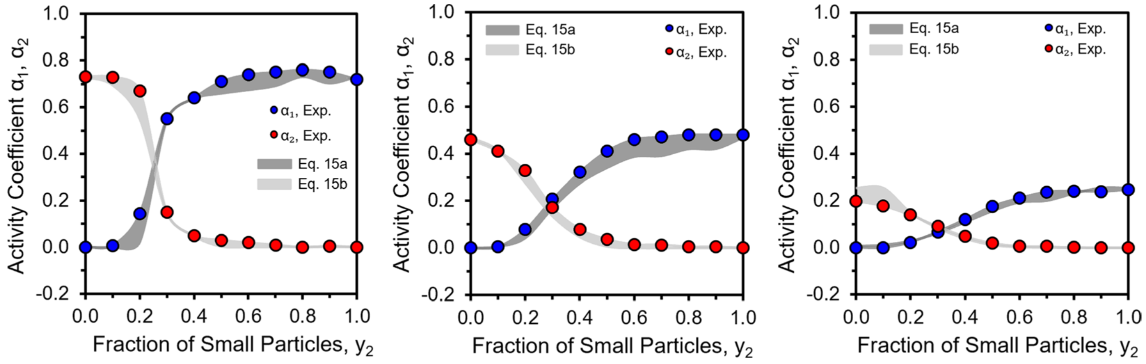

Fig. 6 The activity coefficients calculated from the estimated values of $\bar{x}$

7 Model summary

In Eq. (19), the particle number N_1,N_2 and V are cumbersome to be used due to the huge number of particles of the two species. For practical purpose, unit-less variables are preferred. The volumes $\left(\mathrm{V},\ \mathrm{v}_1^0, \mathrm{v}_2^0, \mathrm{v}_1^g\right)$ can be replaced by specific volumes $(\upsilon, \upsilon_1^0, \upsilon_2^0)$ by using the following relationship: $\mathrm{v}_1^0 = \upsilon_1^0\mathrm{v}_1^g$; $\mathrm{v}_2^0 = \upsilon_2^0\mathrm{v}_2^g$; $V = \upsilon\left(\mathrm{v}_1^g N_1 + \mathrm{v}_2^g N_2\right)$. Note that, by definition, the specific volume can be regarded as the volume potential per unit of solid mass.

The number N_1,N_2 can be expressed in terms of the fractions of particles y_1 and y_2 by Eq. (5). And the volume to be predicted by Eq. (4) can be changed to a more convenient form, given by:

$$\upsilon = \upsilon_1 y_1 + \upsilon_2 y_2 \tag{20}$$

Thus, Eqs. (15), (18) and (19) can be replaced respectively by Eqs. (21), (22), and (23) shown below. The model can be summarized as follows.

Given a bi-dispersed packing specified by $d_1, d_1, \upsilon_1^0, \upsilon_2^0, y_1$ and y_2, the specific volume υ of the bi-dispersed packing can be predicted by the following three equations

$$\upsilon(\bar{x}) = \left(\upsilon_1^0 - \alpha_1(\bar{x})\left(\upsilon_1^0 - 1\right)\right)y_1 + \left(1 - \alpha_2(\bar{x})\right)\upsilon_2^0 y_2 \tag{21}$$

$$\frac{\partial\alpha_1(\bar{x})}{\partial\bar{x}}(\upsilon_1^0 - 1)y_1 + \frac{\partial\alpha_2(\bar{x})}{\partial\bar{x}}\upsilon_2^0 y_2 = 0 \tag{22}$$

$$\alpha_1 = \left(1 - \frac{\bar{x}}{d_1}\right)^\eta; \quad \alpha_2 = \left(1 - \frac{d_2}{\bar{x}}\right)^\eta \tag{23}$$

The solution procedure is as follows.

First, using Eqs. (23) and (22), the unknown variables $\bar{x}$, α_1 and α_2 can be solved. Then, substituting the solved values of α_1 and α_2 into Eq. (21), the specific volume υ of a bi-dispersed packing can be predicted. The value of η is a material parameter, which is calibrated from the measured specific volume υ of one specimen (i.e., a bi-dispersed packing with a particular solid fraction y_2). The calibrated value η can be used to predict the results for bi-dispersed packings made of the same material.

8 Validation with experiments on glass beads

In this section, we evaluate the performance of the model by comparing the model predicted and experimentally measured results on bi-dispersed packings made of glass beads of various fractions and various particle size ratios.

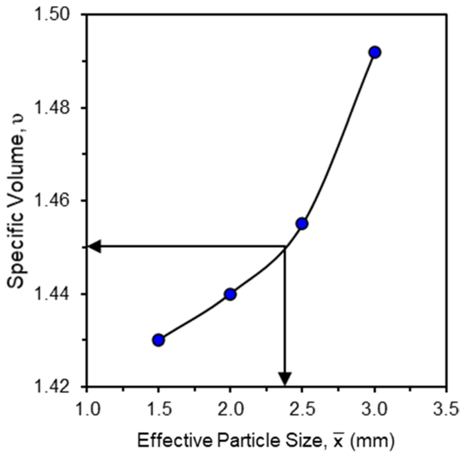

Fig. 7 Trial and error process to calibrate the value of $\eta = 2.4$ using the measure υ (1.45) for the glass beads mixture with $y_2=0.2$

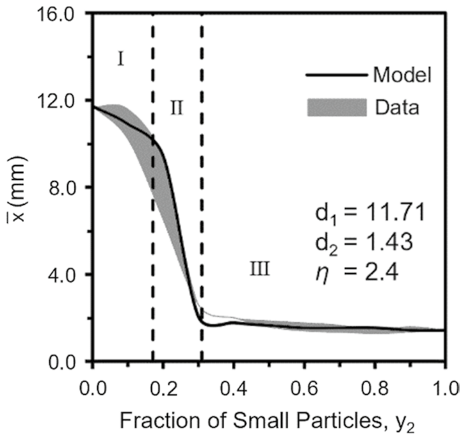

Fig. 8 The model predicted values of $\bar{x}$ for glass beads mixtures with various fractions of small particles y_2

8.1 Glass beads with various fractions of small particles

Experimental measurements obtained from spherical glass beads mixtures, reported by Kwan et al. [35] and described in Sect. 5.1, were selected for model verification. The specific volumes of all bi-mixtures were achieved by a packing preparation procedure specified by British Standard [9]. A bi-dispersed packing is defined by the following parameters $d_1, d_2, \upsilon_1^0, \upsilon_2^0, y_1$ and y_2 (note: $y_1 + y_2 = 1$).

In this validation, specific volumes of nine bi-dispersed specimens were measured with various fractions ($y_2 = 0.1, 0.2, \ldots ..0.9$). The parameters of the bi-dispersed packings are as follows: particle sizes $d_1=11.71$ mm, $d_2=1.43$ mm, the specific volumes for the two species in their mono-dispersed state $\upsilon_1^0=1.706$, $\upsilon_2^0=1.652$.

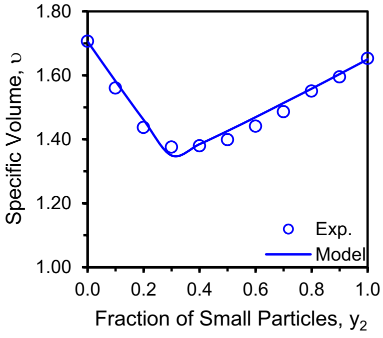

Fig. 9 The predicted specific volume υ for various y_2 compared with the measured results from glass beads mixtures (measured data from Kwan et al. [35]

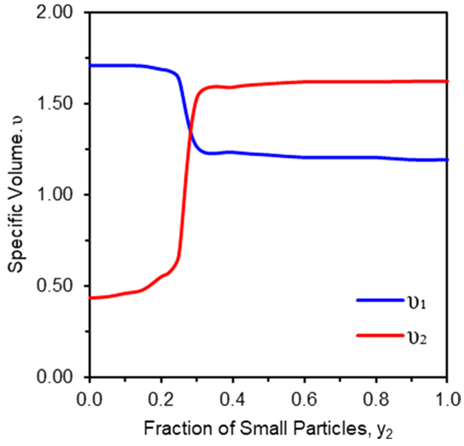

Fig. 10 Predicted specific volumes for the two species. At optimum density $\upsilon_1 = \upsilon_2 = \upsilon = 1.343$

First, we calibrate η using the measured $\upsilon = 1.45$ for the packing mixture with $y_2 = 0.2$. For several trial values of η, the predicted values of υ are plotted in Fig. 7. The calibrated value of η is 2.4. For this specimen at $y_2 = 0.2$, the corresponding value of $x = 9.54$, $\alpha_1 = 0.0175$, and $\alpha_2 = 0.6772$.

Next, we use the calibrated value of $\eta = 2.4$ to predict the specific volumes of the other 8 mixtures with different fractions. The calculated $\bar{x}$ for various fractions of y_2 from the model is plotted in Fig. 8 as a solid line, compared with the back calculated values from measured data (see Sect. 5.1) plotted in Fig. 8 as the shade zone. It shows that the model can predict the $\bar{x}$ values very well using the principle of minimization of excess free volume potential.

The predicted specific volumes υ are shown in Fig. 9 as a solid line, compared with the measured results plotted as circular symbols. This figure shows a very good agreement between prediction and measured results.

It is note that the specimen, with the lowest predicted volume (i.e., optimum density), has a fraction of $y_2 = 0.28$. The prediction agrees with the measured results. The trend of V shape for the variation of υ versus y_2 is also captured by the model. It is noted that at the lowest value of specific volume, the derivative of υ in Eq. (20) with respect to y_2 is zero, i.e., $\frac{\partial \upsilon}{\partial y_2} = 0$. According to Eq. (20), this derivative leads to $\upsilon_1 = \upsilon_2$. Thus, at the condition of optimum density, the specific volumes of the two species are equal. The predicted specific volumes for both species are shown in Fig. 10. It shows that, at the point of optimum density, $y_2 = 0.28$, $\bar{x} = 2.842$, the specific volumes for both species are also equal to the specific volume of packing mixture (i.e., $\upsilon_1 = \upsilon_2 = \upsilon = 1.343$). Note that at the optimum density, the activity coefficients are not equal; $\alpha_1 = 0.513$, and $\alpha_2 = 0.186$.

8.2 Glass beads with various particle size ratios

We further probe the predictive power of our model for bi-dispersed packings with different ratios of particle sizes. The experimental results obtained by Kwan et al. [35] for three

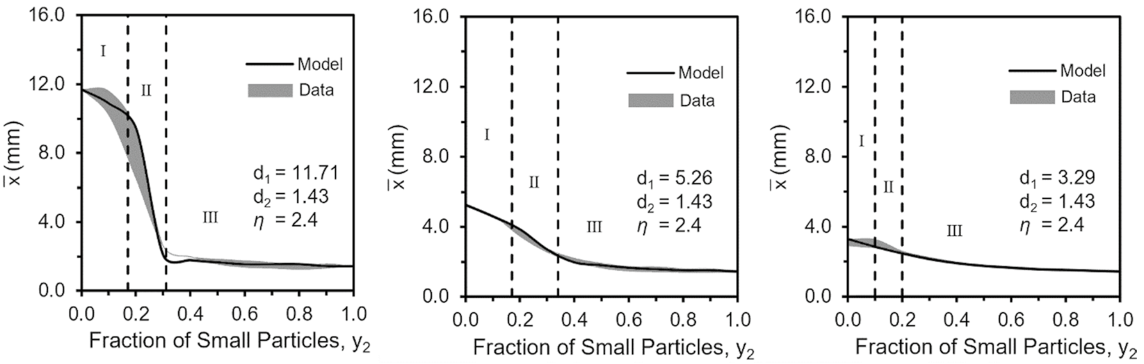

Fig. 11 The model predicted values of $\bar{x}$ vs y_2 for the three glass beads mixtures with different size ratios

systems of bi-dispersed packing (see Sect. 6.1), are used for this validation.

Since all packings were made of same types of spherical glass beads, we use the same value of $\eta = 2.4$. Using Eqs. (21–23), the calculated $\bar{x}$ vs y_2 are shown in Fig. 11 for the three systems (i.e. three size ratios) of bi-dispersed particle mixtures. Each system of a given size ratio contains nine packing mixtures (with fractions $y_2 = 0.1, 0.2, \ldots .0.9$), total 27 specimens for the three systems.

Figure 11 shows that, for all three size ratios, the model predicted $\bar{x}$ (shown as solid lines) fit well with those back calculated from experiment (shown as shaded zone). The variation of $\bar{x}$ also show three regions that governs the characteristics of microstate configurations. The predicted specific volumes for the three bi-dispersed systems are shown in Fig. 12, which are in good agreement with the measured results.

The model also correctly predicts the magnitudes and the species fractions of the optimum densities for the three bi-dispersed systems. It is noted that all 27 predictions were made by using only one parameter $\eta = 2.4$. It demonstrates that the proposed simple model has captured the underlying physics of granular compaction of a bi-dispersed packing.

9 Validation with experiments on sand mixtures

The experiments used for model verification in the previous section were obtained from man-made glass beads. In this section, the validation will be carried out using silica sand, which involve particles of non-spherical shape and different surface texture, compared with glass beads.

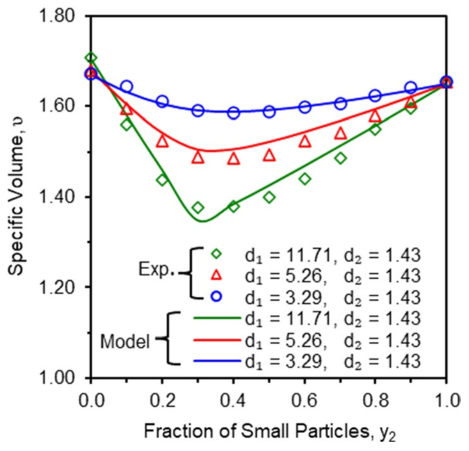

Fig. 12 The predicted specific volumes for various y_2 for three glass beads mixtures compared with the measured results (data from Kwan et al. [35])

Experimental results for a soil mixture (Silica#16-#18 #50-#80) reported by Yilmaz [59] were selected for model verification. The two size-groups of sand were obtained from sieving sand through standard sieves. It is noted that, due to the angular shape of sand, in each species, the sizes and shapes of sand grains are not exactly the same. The specific volumes of all silica sand mixtures were achieved by a sample preparation procedure specified by ASTM D4253 [3]. The system of bi-dispersed packings of the silica sand is defined by four parameters: $d_1 = 1.08$ mm, $d_2 = 0.263$ mm, $\upsilon_1^0 = 1.633$, $\upsilon_2^0 = 1.696$. The aim now is to compare the predicted and measured specific volumes for packing mixtures with various y_2.

First, the test result of $\upsilon = 1.47$ for $y_2 = 0.2$ is used for the calibration of parameter η. Following the same trial

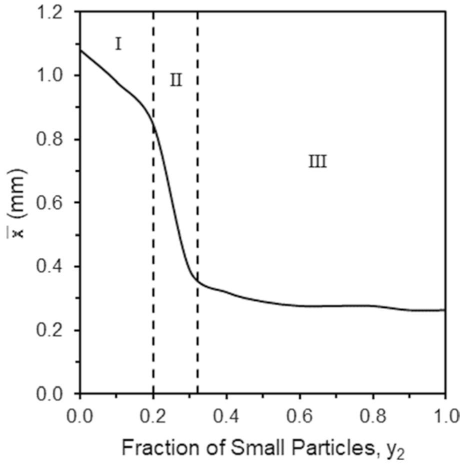

Fig. 13 The model predicted $\bar{x}$ for the silica sand mixtures with various fractions of small particles y_2

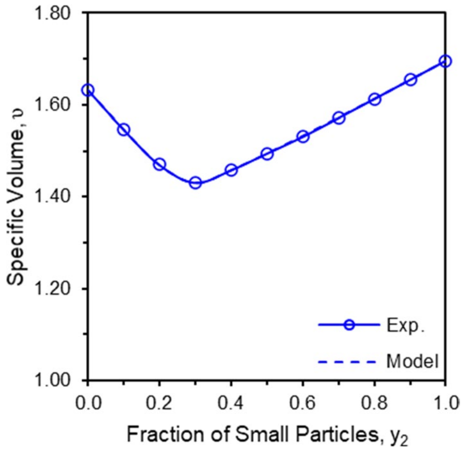

Fig. 14 The predicted specific volumes for various fractions y_2 compared with the measured results from silica sand mixtures (data reported by Yilmaz [59])

and error process, the calibrated value of η is 2.1 for the bi-dispersed packings of silica sand mixtures. Note that, for spherical glass beads, the value of $\eta = 2.4$. The particles for silica sand are sub-angular in shape.

Using $\eta = 2.1$, the calculated internal state variable $\overline{x}$ for various y_2 is plotted in Fig. 13.

The calculated $\overline{x}$ has a similar shape with that obtained for glass beads. It also shows three zones for the characteristics of microstate configurations. The underlying physics are similar between glass beads and sand. The model predicted specific volumes are shown in Fig. 14 as a dashed line, compared with the measured results plotted as circle symbols. This figure shows a very good agreement between prediction and measured results.

This prediction method is then applied to predict 24 sets of sand mixtures listed in Table 1. There is one material parameter η corresponding to each type of sand mixture of various fractions of small particles y_2. The calibrated value of η is expected to be influenced by the shape and surface textures of sand particles. The value of η is from 2.0 to 5.5 for natural sand as listed in Table 1. The comparisons between prediction and measurements for the 24 types of mixtures are shown in Fig. 15, which demonstrated an overall good agreement. Therefore, the proposed model is applicable to natural sand.

10 Conclusion

Analogic similarities are drawn between the chemical potentials of a solution with two species and the volume potentials of a granular mixture with two components. Following the Edwards' approach by replacing energy with volume in thermodynamics, we build a simple model to predict the specific volume of bi-dispersed granular packing. We introduced an internal state variable to represent the state of packing configuration, which leads to a simple method of describing the excess free volume potential by considering the interaction activity between the two species in a bi-dispersed packing. We also use the principal of minimum excess free volume potential to determine the activity coefficients. The

Table 1 List of material properties for 24 sets of bi-dispersed granular soil mixtures

Sand/silt mixture	References	d_1 (mm)	d_2 (mm)	υ_1^0	υ_2^0	Large particle shape	Small particle shape	η
Ottawa 50/200-Nevada fines	Lade and Yamamuro [37]	0.2	0.05	1.548	1.754	Angular	Angular	2.4
Ottawa F95-Nevada fines		0.16	0.05	1.580	1.754	Subrounded	Angular	2.6
Nevada 50/200-Nevada fines		0.14	0.04	1.570	1.754	Subangular	Angular	2.3
Nevada 50/80-Nevada fines	Lade et al. [36]	0.21	0.05	1.581	1.754	Subangular to angular	Subangular to angular	2.7
Nevada 80/200-Nevada fines		0.12	0.05	1.617	1.754	Subangular to angular	Subangular to angular	3.0
Nevada 50/80-Nevada80/200 + fines		0.17	0.05	1.581	1.754	Subangular to angular	Subangular to angular	3.0
Hokksund	Yang [57]	0.45	0.04	1.570	1.760	Sharp edges, cubical	Angular, subangular	4.2
MGM	Fourie and Papageorigou [24]	0.12	0.01	1.755	2.000	Angular to subrounded	Thin and plate-like	4.3
Vietnam	Cho [12]	0.37	0.16	1.552	1.583	Subangular	Subangular	2.5
Cambria-Nevada fines	Lade et al. [36]	1.5	0.05	1.538	1.754	Rounded	Angular	5.5
Cambria-Nevada 50/80		1.5	0.21	1.538	1.581	Rounded	Subangular	3.1
Cambria-Nevada 80/200		1.5	0.12	1.538	1.624	Rounded	Angular	4.2
Nevada 50/80- Nevada 80/200		0.21	0.12	1.581	1.617	Subangular to angular	Subangular to angular	2.1
Foundry sand/crushed silica fines	Thevanayagam et al. [54]	0.25	0.01	1.608	1.627	Rounded to subrounded	Angular	5.5
Silica#16-#18 #30-#50	Yilmaz [59]	1.08	0.4	1.633	1.644	Subangular	Subangular	2.0
Silica#16-#18 #30-#80		1.08	0.42	1.633	1.590	Subangular	Subangular	2.0
Silica#16-#18 #50-#80		1.08	0.26	1.633	1.696	Subangular	Subangular	2.1
Silica#16-#18 #80-#100		1.08	0.17	1.633	1.682	Subangular	Subangular	2.1
Silica#16-#18 #80-#120		1.08	0.14	1.633	1.697	Subangular	Subangular	2.1
Silica#16-#18 #80-#200		1.08	0.1	1.633	1.651	Subangular	Subangular	2.1
Silica#16-#18 #100-#120		1.08	0.14	1.633	1.697	Subangular	Subangular	2.1
Silica#16-#18 #100-#200		1.08	0.1	1.633	1.668	Subangular	Subangular	2.1
Silica#16-#18 #120-#200		1.08	0.1	1.633	1.682	Subangular	Subangular	2.4
Silica#16-#18 #200-#400		1.08	0.06	1.633	1.700	Subangular	Subangular	2.4

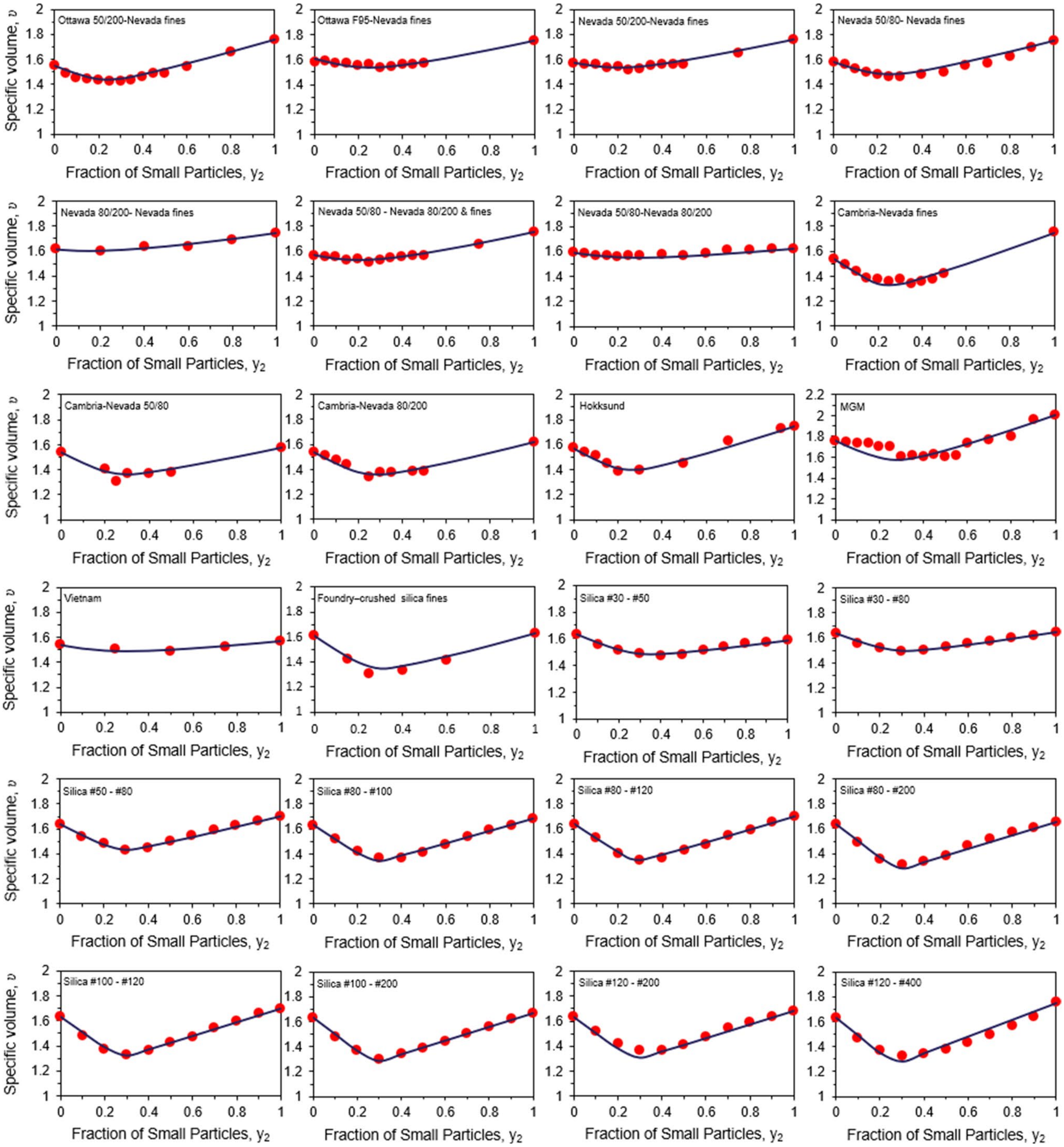

Fig. 15 The comparison between prediction and measure specific volumes for the 24 types of bi-dispersed granular soil mixtures

model only requires one calibrated parameter for the type of material.

Using the proposed model, the predicted results are in excellent agreement with the experimental data on glass beads and on 24 types of natural sand. These results validate the model as a tool for predicting the effects of bidispersity on random packings. The model performance demonstrates that the model, based on thermodynamics theory, can capture the correct underlying physics of granular compaction of bi-dispersed packings.

Acknowledgements This work was supported by the National Science Foundation of the United States under a research grant (CMMI-1917238). The support is greatly acknowledged.

Declarations

Conflict of interest The authors declare that they have no conflict of interest.

References

1. An, X.Z.: Densification of the packing structure under vibrations. Int. J. Miner. Metall. Mater. **20**, 499–503 (2013). https://doi.org/10.1007/s12613-013-0757-9
2. Aste, T., Saadatfar, M., Senden, J.T.: Local and global relations between the number of contacts and density in monodisperse sphere packs. J. Stat. Mech. (2006). https://doi.org/10.1088/1742-5468/2006/07/P07010
3. ASTM D4253-00: Standard test methods for maximum index density and unit weight of soils using a vibratory table. In: Annual Book of ASTM Standards. ASTM International, West Conshohocken, pp. 1–15 (2006). https://doi.org/10.1520/D4253-00R06
4. Atkins, P., dePaula, J.: Section 5.9, the activities of ions in solution. In: Physical Chemisrry, 8th edn. OUP. ISBN: 9780198700722 (2006)
5. Baule, A., Morone, F., Herrmann, H.J., Makse, H.A.: Edwards statistical mechanics for jammed granular matter. Rev. Mod. Phys. **90**, 15006 (2018). https://doi.org/10.1103/RevModPhys.90.015006
6. Blumenfeld, R., Amitai, S., Jordan, J., Hihinashvili, R.: Failure of the volume function in granular statistical mechanics. Phys. Rev. Lett. **116**, 148001 (2016)
7. Blumenfeld, R., Edwards, S.: Geometric partition functions of cellular systems: explicit calculation of the entropy in two and three dimensions. Eur. Phys. J. E **19**, 23–30 (2006)
8. Blumenfeld, R., Edwards, S.F.: On granular stress statistics: compactivity, angoricity, and some ppen issues. J. Phys. Chem. B **113**, 3981–3987 (2009). https://doi.org/10.1021/jp809768y
9. BS 182: Testing Aggregates Part 2: Methods of Determination of Density. British Standards Institution (1995)
10. Chang, C.S., Deng, Y.: A particle packing model for sand–silt mixtures with the effect of dual-skeleton. Granul. Matter (2017). https://doi.org/10.1007/s10035-017-0762-1
11. Cheng, G., Yu, A., Zulli, P.: Evaluation of effective thermal conductivity from the structure of a packed bed. Chem. Eng. Sci. **54**, 4199–4209 (1999)
12. Cho, Y.T.: The Study of GCTS Triaxial Apparatus Function and Mixing Sand Void Ratio. National Taiwan University (2014)
13. Clarke, A.S., Wiley, J.D.: Numerical simulation of the dense random packing of a binary mixture of hard spheres: amorphous metals. Phys. Rev. B **35**, 7350–7356 (1987). https://doi.org/10.1103/PhysRevB.35.7350
14. Coleman, B., Gurtin, M.: Thermodynamics with internal state variables. J. Chem. Phys. **47**, 597 (1967). https://doi.org/10.1063/1.1711937
15. da Cruz, F., Lechenault, F., Dauchot, O., Bertin, E.: Free volume distributions inside a bidimensional granular medium. In: Herrmann, H.J., Garcia-Rojo, R., McNamara, S. (eds.) Powders and Grains 2005. CRC Press, Stuttgart (2005)
16. Danisch, M., Jin, Y., Makse, H.A.: Model of random packings of different size balls. Phys. Rev. E **81**, 051303 (2010). https://doi.org/10.1103/PhysRevE.81.051303
17. De Larrard, F.: Concrete Mixture Proportioning: A Scientific Approach. E & FN SPON, London (1999)
18. Desmond, K.W., Weeks, E.R.: Influence of particle size distribution on random close packing of spheres. Phys. Rev. E **90**, 022204 (2014). https://doi.org/10.1103/PhysRevE.90.022204
19. Dewar, J.D.: Computer Modelling of Concrete Mixtures. E & FN Spon, London (1999)
20. Dutt, M., Elliott, J.A.: Granular dynamics simulations of the effect of grain size dispersity on uniaxially compacted powder blends. Granul. Matter **16**, 243–248 (2014). https://doi.org/10.1007/s10035-013-0463-3
21. Edwards, S.F.: New kinds of entropy. J. Stat. Phys. **116**, 29–42 (2004). https://doi.org/10.1023/B:JOSS.0000037233.36686.2f
22. Edwards, S.F., Grinev, D.V.: Compactivity and transmission of stress in granular materials. Chaos **9**, 551–558 (1999). https://doi.org/10.1063/1.166429
23. Edwards, S.F., Oakeshott, R.B.S.: Theory of powders. Physica A **157**, 1080–1090 (1989). https://doi.org/10.1016/0378-4371(89)90034-4
24. Fourie, A.B., Papageorigou, G.: Defining an appropriate steady state line for Merriespruit gold tailings. Can. Geotech. J. **38**, 695–706 (2001). https://doi.org/10.1139/cgj-38-4-695
25. Fuggle, A.R., Roozbahani, M.M., Frost, J.D.: Size effects on the void ratio of loosely packed binary particle mixtures. In: Abu-Farsakh, M., Yu, X., Hoyos, L.R. (eds.) Geo-Congress 2014 Technical Papers, pp. 129–138. American Society of Civil Engineers, Atlanta (2014). https://doi.org/10.1061/9780784413272.014
26. Ge, X., Wang, X., Zhang, M., Seetharaman, S.: Correlation and prediction of activity and osmotic coefficients of aqueous electrolytes at 298.15 K by the modified TCPC model. J. Chem. Eng. Data **52**(2), 538–547 (2007). https://doi.org/10.1021/je060451k.ISSN0021-9568
27. Goltermann, P., Johansen, V., Palbøl, L.: Packing of aggregates: an alternative tool to determine the optimal aggregate mix. ACI Mater. J. **94**, 435–443 (1997)
28. Holtz, R.D., Kovacs, W.D., Sheahan, T.C.: An Introduction to Geotechnical Engineering, 2nd edn. Pearson, Upper Saddle River (2011)
29. Hopkins, A.B., Stillinger, F.H., Torquato, S.: Disordered strictly jammed binary sphere packings attain an anomalously large range of densities. Phys. Rev. E **88**, 022205 (2013). https://doi.org/10.1103/PhysRevE.88.022205
30. Horstemeyer, M., Bammann, D.: Historical review of internal state variable theory for inelasticity. Int. J. Plast. **26**(9), 1310–1334 (2010). https://doi.org/10.1016/j.ijplas.2010.06.005
31. Jalali, P., Li, M.: Model for estimation of critical packing density in polydisperse hard-disk packings. Physica A **381**, 230–238 (2007). https://doi.org/10.1016/j.physa.2007.03.024
32. Jin, Y., Makse, H.A.: A first-order phase transition defines the random close packing of hard spheres. Physica A (Amsterdam) **389**, 5362 (2010)
33. Kelly, E.G., Spottiswood, D.J.: Introduction to Mineral Processing. Wiley, New York (1982)
34. Kumar, N., Magnanimo, V., Ramaioli, M., Luding, S.: Tuning the bulk properties of bidisperse granular mixtures by small amount of fines. Powder Technol. **293**, 94–112 (2016). https://doi.org/10.1016/j.powtec.2015.11.042
35. Kwan, A.K.H., Chan, K.W., Wong, V.: A 3-parameter particle packing model incorporating the wedging effect. Powder Technol. **237**, 172–179 (2013). https://doi.org/10.1016/j.powtec.2013.01.043

36. Lade, P.V., Liggio, C.D., Yamamuro, J.A.: Effects of non-plastic fines on minimum and maximum void ratios of sand. Geotech. Test. J. **21**, 336–347 (1998). https://doi.org/10.1520/GTJ11373J
37. Lade, P.V., Yamamuro, J.A.: Effects of nonplastic fines on static liquefaction of sands. Can. Geotech. J. **34**, 918–928 (1997). https://doi.org/10.1139/t97-052
38. Lange, K.D., Wouterse, A., Philipse, A.: Simulation of random packing of binary sphere mixtures by mechanical contraction. Phys. A Stat. Mech. Appl. **358**, 249–262 (2005). https://doi.org/10.1016/j.physa.2005.03.057
39. Liu, W., Li, S., Baule, A., Makse, H.A.: Adhesive loose packings of small dry particles. Soft Matter **11**(32), 6492–6498 (2015)
40. Martin, C.L., Bouvard, D.: Isostatic compaction of bimodal powder mixtures and composites. Int. J. Mech. Sci. **46**, 907–927 (2004). https://doi.org/10.1016/j.ijmecsci.2004.05.012
41. Maugin, G.A.: The Thermomechanics of Plasticity and Fracture. Cambridge University Press, Cambridge (1992)
42. Meyer, S., Song, C., Jin, Y., Wang, K., Makse, H.: Jamming in two-dimensional packings. Physica (Amsterdam) **389**, 5137 (2010)
43. Muzzio, F.J., Shinbrot, T., Glasser, B.J.: Powder technology in the pharmaceutical industry: the need to catch up fast. Powder Technol. **124**, 1–7 (2002). https://doi.org/10.1016/S0032-5910(01)00482-X
44. Nowak, E.R., Knight, J.B., Ben-Naim, E., Jaeger, H.M., Nagel, S.R.: Density fluctuations in vibrated granular materials. Phys. Rev. E **57**, 1971–1982 (1998). https://doi.org/10.1103/PhysRevE.57.1971
45. Ogarko, V., Luding, S.: Prediction of polydisperse hard-sphere mixture behavior using tridisperse systems. Soft Matter **9**, 9530–9534 (2013). https://doi.org/10.1039/c3sm50964h
46. Rhodes, M.: Introduction to Particle Technology, 2nd edn. Wiley, West Sussex (2008)
47. Rockwood, A.L.: Meaning and measurability of single-ion activities, the thermodynamic foundations of pH, and the Gibbs free energy for the transfer of ions between dissimilar materials. ChemPhysChem **16**(9), 1978–1991 (2015). https://doi.org/10.1002/cphc.201500044.ISSN1439-4235.PMC4501315.PMID25919971
48. Roquier, G.: The 4-parameter Compressible Packing Model (CPM) including a new theory about wall effect and loosening effect for spheres. Powder Technol. **302**, 247–253 (2016). https://doi.org/10.1016/j.powtec.2016.08.031
49. Santiso, E., Müller, E.: Dense packing of binary and polydisperse hard spheres. Mol. Phys. **100**, 2461–2469 (2002). https://doi.org/10.1080/00268970210125313
50. Skrinjar, O., Larsson, P.: On discrete element modelling of compaction of powders with size ratio. Comput. Mater. Sci. **31**, 131–146 (2004). https://doi.org/10.1016/j.commatsci.2004.02.005
51. Song, C., Havlin, S., Makes, H.A.: Self-similarity of complex networks. Nature **433**(7024), 392–395 (2005)
52. Song, C., Wang, P., Makse, H.A.: A phase diagram for jammed matter. Nature (London) **453**, 629 (2008)
53. Stovall, T., de Larrard, F., Buil, M.: Linear packing density model of grain mixtures. Powder Technol. **48**, 1–12 (1986). https://doi.org/10.1016/0032-5910(86)80058-4
54. Thevanayagam, S., Shenthan, T., Mohan, S., Liang, J.: Undrained fragility of clean sands, silty sands, and sandy silts. J. Geotech. Geoenviron. Eng. **128**, 849–859 (2002). https://doi.org/10.1061/(ASCE)1090-0241(2002)128:10(849)
55. Ueda, T., Matsushima, T., Yamada, Y.: Effect of particle size ratio and volume fraction on shear strength of binary granular mixture. Granul. Matter **13**, 731–742 (2011). https://doi.org/10.1007/s10035-011-0292-1
56. Voivret, C., Radjaï, J., Delenne, J.-Y., Youssoufi, M.S.E.: Space-filling properties of polydisperse granular media. Phys. Rev. E **76**, 021301 (2007). https://doi.org/10.1103/PhysRevE.76.021301
57. Yang, S.L.: Characterization of the Properties of Sand–Silt Mixtures. Norwegian University of Science and Technology (2004)
58. Yi, L.Y., Dong, K.J., Zou, R.P., Yu, A.B.: Radical tessellation of the packing of ternary mixtures of spheres. Powder Technol. **224**, 129–137 (2012). https://doi.org/10.1016/j.powtec.2012.02.042
59. Yilmaz, Y.: A study on the limit void ratio characteristics of medium to fine mixed graded sands. Eng. Geol. **104**, 290–294 (2009). https://doi.org/10.1016/j.enggeo.2008.11.009
60. Yu, A.B., Standish, N.: An analytical-parametric theory of the random packing of particles. Power Technol. **55**, 171–186 (1988). https://doi.org/10.1016/0032-5910(88)80101-3
61. Yu, A.B., Standish, N.: Porosity calculations of multi-component mixtures of spherical particles. Powder Technol. **52**, 233–241 (1987). https://doi.org/10.1016/0032-5910(87)80110-9